DIRECTIONAL RETURN PULSE CHARACTERIZATION

R M Gott (1), A B Martinez (1), B S Bourgeois (2), E J Kaminsky (3)

(1) Tulane University, EE Dept., New Orleans, LA, USA.
(2) Naval Research Laboratory, Stennis Space Center, MS, USA.
(3) Sverdrup Technology, Stennis Space Center, MS, USA.

1. INTRODUCTION

Multibeam sonar systems such as the Sonar Array Survey System (SASS) ensonify an area of the bottom of the ocean, not a single point, and the returned energy spans a finite time. In the SASS data processing, beamforming is used to discriminate the returning sonar energy into angular components, or beams. A Fast Fourier Transform (FFT) algorithm is used in the beamforming process, which yields an array of intensities (an intensity for each beamformer bin and sample time) returned by the source, usually the bottom of the ocean. The peaks of the envelopes of the beamformed signal correspond to the intersection of the Maximim Response Axis (MRA) and the area ensonified. In order to accurately calculate the distance from the source to the ship, and from it the bathymetry, the time t_c corresponding to the center of a beam needs to be determined. One method used for determination of the MRA time is matched filtering. Here, the received time signal (the output of the beamformer) is low-pass filtered, and the peak of the smoothed curve is then detected. This smoothed curve represents the pulse shape of the bottom return as a function of time. A filter is computed for each bin of the ping being processed. Although a Rician model has been proposed in [1] as being a closer match to the pulse shape, a Gaussian model is often used [1, 2]. This paper investigates if the Gaussian assumption for the shape of the bottom return is accurate for SASS data. The filter that most closely matches the return signal yields the most accurate results in determination of t_c; such a filter is therefore desired.

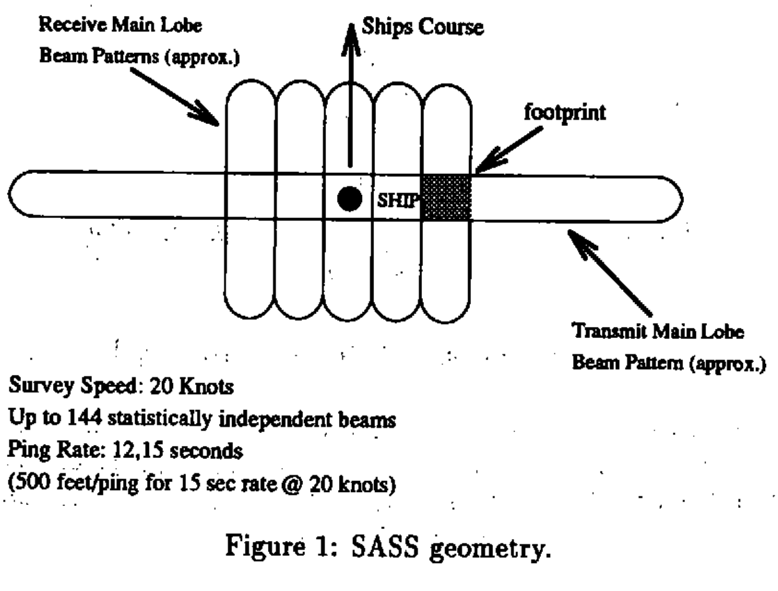

Figure 1: SASS geometry.

2. SYSTEM AND DATA DESCRIPTION

The Sonar Array Survey System (SASS), operated by the Naval Oceanographic Office (NAVOCEANO), is a hull-mounted system with a linear array of 144 hydrophones. SASS is a multibeam system that is able to map with high resolution a large swath of the seafloor with each transmit pulse, as shown in Fig. 1. The system transmits at 12KHz and records the in-phase and quadrature voltages off the hydrophones every 3 msec. The SASS projector array insonifies the bottom of the ocean with a narrow beam of approximately one degree directed perpendicular to the ship's heading. The system receives the echo with 144 receiver hydrophones that are mounted athwartships (perpendicular to the projector), and spaced $\lambda/2$ apart, where λ is the nominal wavelength [2]. The SASS system has historically been used for bathymetry only; however, there is more information that can be extracted from the SASS data. The raw SASS data may be processed to produce bathymetry, side-scan imagery, and textured images.

The data from 283 pings of a SASS mission are used in the analysis presented in this paper. As seen in Fig. 2, the actual return is noisy, exhibitting deep nulls and fluctuations. It is therefore necessary to low-pass filter the data to extract the smooth pulse shape of the return. We use a third order Butterworth filter to smooth the SASS data. Fig. 2 also shows the filtered version of a return.

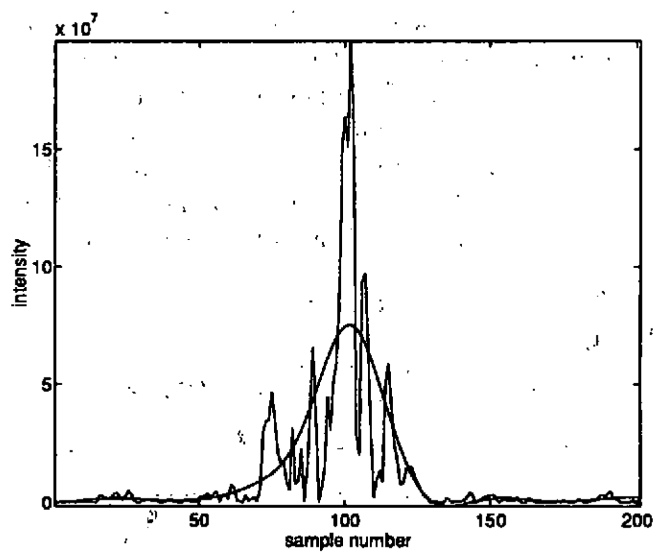

Figure 2: Unfiltered and filtered return signal.

The work presented uses tools from statistical analysis to determine an accurate shape for the return pulse as a function of time. We will investigate functional forms of Gaussian and Rician probability density functions (pdfs) to characterize the shape of the return, but do not actually classify the distribution of intensities of the signal as such.

3. MATCHED FILTER DESIGNS

Matched filtering techniques have been proposed and studied [1, 3] as an accurate method for determining the beam's center time, t_c. Other methods are studied in [4]. Current SASS processing at the Naval Research Laboratory (NRL) employs a Gaussian filter to match to the return signal. The width of the filter is given by the number of samples which exceed a signal-to-noise (SNR) dependent threshold. The Gaussian filter is a scaled version of the functional form of the Gaussian pdf with zero mean and variance σ^2, and is given in [2] by:

$$y = \exp\left[-\frac{1}{2}\left(\frac{x}{\sigma}\right)^2\right] \tag{1}$$

Both the Rayleigh and Rician distributions have been used to characterize the envelope of the bottom return signal [5]. Morgera [1] presents a model of the envelope of the bottom return using the functional form of the Rician pdf. Here, the expected bottom return envelope of a multibeam sonar system signal received from various spatial directions is modeled as a smooth nearly Gaussian-shaped function for near-nadir steering angles and as a nearly Rayleigh-shaped function for off-vertical angles. The model is a deterministic function where the shape is dependent on the steering angle Φ, the depth d, and pulse length τ. Fig. 3 shows examples of envelopes generated using the Rician model for steering angles of 15, 30, and 45 degrees.

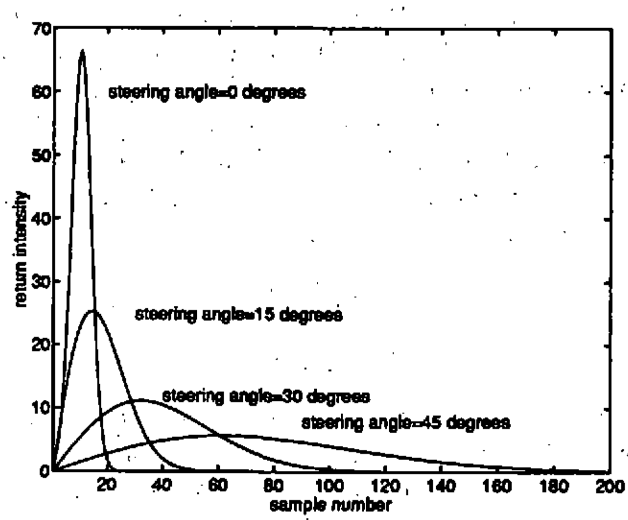

Figure 3: Smooth bottom function.

Morgera uses the following approximation for the functional form of the Rician pdf:

$$s(k) = \begin{cases} \frac{r}{\sigma^2}\exp\left(-\frac{r^2}{2\sigma^2}\right), & S \ll 1 \\ \frac{1}{\sqrt{2\pi}\sigma}\exp\left[-\frac{(r-E_c)^2}{2\sigma^2}\right] & S \gg 1 \end{cases} \tag{2}$$

where $S = E_c^2/2\sigma^2$. The parameters E_c and σ in (2) were chosen to be

$$E_c = \tau[\exp(\cos\phi) - 1] \tag{3}$$

$$\sigma = \alpha T(\phi, d) \tag{4}$$

where the approximate values of α used are 0.6 close to nadir and 0.8 off nadir. T is the expected echo duration given by

$$T(\phi, d) \approx \frac{2d\theta}{c} \tan\phi \sec\phi + \tau \tag{5}$$

with d the depth, ϕ the steering angle, c the speed of sound in water, τ the time duration of the transmitted signal, and θ the receive beamwidth in radians.

For $S \ll 1$ (corresponding to larger steering angles) the output Rician pdf approximates a Rayleigh pdf, and for $S \gg 1$ (corresponding to near-vertical steering angles) the Rician pdf approximates a Gaussian pdf. The curves between these two extremes yield a smooth envelope of the received signal given the variation of certain bottom parameters. The smooth envelope given by the Rician pdf can then be used for matched filtering of the return signal [1].

4. STATISTICAL ANALYSIS

We describe in this section the statistical based analysis used to characterize the return pulse's shape. The method of moments is employed to fit the pulse shape to a known distribution. The filtered pulse shape is treated as if it were a pdf when calculating the moments in order to fit the pulse shape to a distribution curve. In the method of moments, the first four moments of the data (the filtered pulse shape) are caluclated, and then used to select a suitable theoretical curve that matches its shape. The first four moments, μ_1, μ_2, μ_3, and μ_4, were calculated for the data, from which the skewness β_1 and kurtosis β_2 can be found:

$$\beta_1 = \mu_3^2/\mu_2^3 \tag{6}$$

$$\beta_2 = \mu_4/\mu_2^2 \tag{7}$$

For the Gaussian distribution is a single point at $\beta_1 = 0$ and $\beta_2 = 3$. For 'nearly' Gaussian distributions, $\beta_1 \leq 0.1$ and $2.62 \leq \beta_2 \leq 3.42$ [6]. Ol'shevskii [5] develops an expression for the skewness of the Rician pdf showing (in terms of Morgera's model) as $S \to \infty$ the value of $\beta_1 \to 0$. This corresponds to the Gaussian characteristics at near-vertical steering angles.

The Pearson system is a family of distributions which includes special cases of Gaussian, Cauchy, t, F, χ^2, γ, exponential, and β densities. The Pearson family offers solutions to the differential equation

$$\frac{f'(x)}{f(x)} = \frac{a + x}{b_0 + b_1 x + b_2 x^2} \tag{8}$$

and is used as a tool for fitting data to densities.

Table 1: Pearson Family Main Types.

Type	Equation	Range	Associated Distribution
	Main		
I	$K(1+x/\alpha_1)^{\nu\alpha_1}(1-x/\alpha_2)^{\nu\alpha_2}$	$[-\alpha_1, \alpha_2]$	beta, F
IV	$K(1+x^2/\alpha^2)^{-m}\exp[-\nu\tan^{-1}(x/\alpha)]$	$(-\infty, \infty)$	
VI	$K(x-\alpha)^{m_2}x^{-m_1}$	$[\alpha, \infty)$	Pareto, F, Lomax
	Transition		
Gaussian	$K\exp[-x^2/2\sigma^2]$	$(-\infty, \infty)$	
II(I)	$K(1-x^2/\alpha^2)^m$	$[-\alpha, \alpha]$	beta
VII(IV)	$K(1+x^2/\alpha^2)^{-m}$	$(-\infty, \infty)$	t, Cauchy

The three main types in the Pearson family depend on the roots of the denominator of (8), of which there are three possibilities: 1) real roots, same sign, 2) real roots, different signs, and 3) complex conjugate roots, corresponding to the Pearson three main types VI, I, and IV respectively. Transition types are encountered when parameters of the main types approach their limiting values [6]. The type I family borders the limiting values for all densities. The first four moments of a pdf can be used to find the coefficients for the Pearson system. The Pearson family main types and three of the transition types are summarized in Table 1 and shown in Fig. 4. In this figure type VII corresponds to the vertical axis ($\beta_1 = 0$) for β_2 values greater than 3 (gaussian). Type II corresponds to the small region of the vertical axis below $\beta_2 = 3$ and above the limiting value of region I.

The criteria κ, given by

$$\kappa = \frac{\beta_1(\beta_2+3)^2}{4(2\beta_2-3\beta_1-6)(4\beta_2-3\beta_1)} \tag{9}$$

also characterizes the different types in the Pearson family. Type IV requires $0 < \kappa < 1$ and transition types Gaussian, II, and VII require $\kappa = 0$. Examples of these densities are shown in Figs. 5 and 6. In Fig. 5 increasing β_1 skews the density curve to the right, and increasing β_2 sharpens the curve. In Fig. 6 β_1 has no effect but β_2 causes a similar sharpening effect.

5. RESULTS AND CONCLUSIONS

Values of skewness and kurtosis for a representative subset of data are plotted in Fig. 4. The SASS data lies primarily in the type IV region (skewed and bell-shaped curves), and on the types II, VII (symmetric and usually bell-shaped curves) and normal (Gaussian) transitions. The skewed nature of many of the SASS pulse shapes makes the Gaussian filter inadequate for precise matched filtering. Reasonable results may be yielded with this method since many of the returns are symmetric in nature, but the Rician filter offers a more robust solution. The Rician pdf approximates the Gaussian pdf at near-vertical steering angles.

Fig. 7 shows κ values for the filtered SASS data. Bins 95-165 correspond roughly to steering angles of $-15°$ to $15°$. The criteria $\kappa = 0$ for this range indicates symmetric densities of types II, VII, and

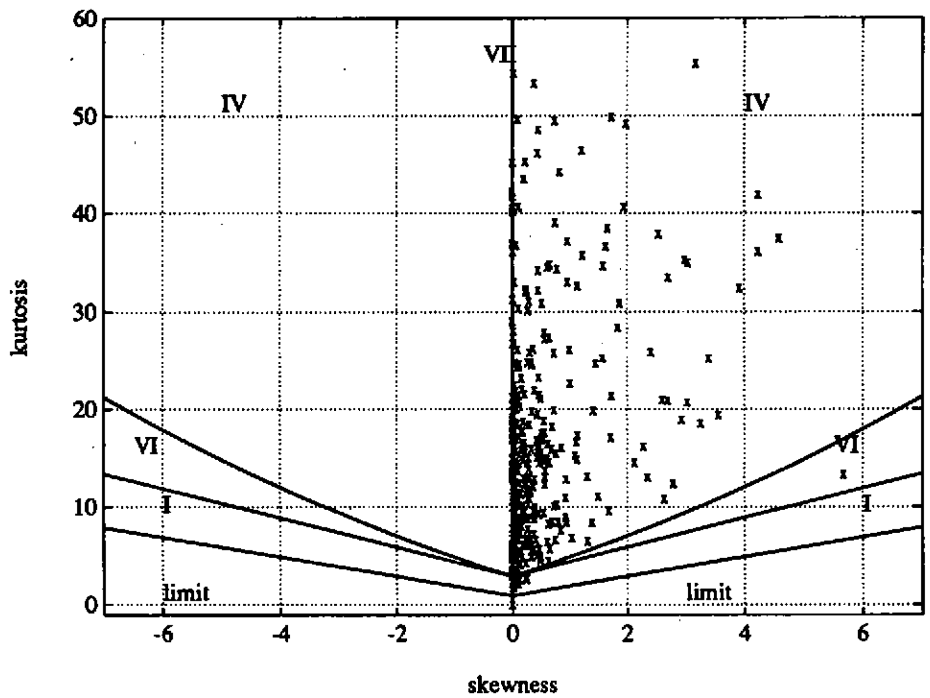

Figure 4: Pearson Densities in a B1 x B2 plane of filtered SASS data.

normal. Hence, a Gaussian-shaped filter would be appropriate for this range of steering angles. Bins 35-95 and 165-225 correspond to steering angles of $-45°$ to $-15°$ and $15°$ to $45°$, respectively. The criterion κ takes on values $0 < \kappa < 1$ in this range, fufilling the type IV requirement. Type IV curves are skewed and bell-shaped. The Rician pdf approximates the Rayleigh pdf at the higher steering angles, which is appropriate for the skewed nature of the type IV density. Bins 0-35 and 225-255 correspond to the extreme steering angles. Many of the returns in this range are dropouts and were not used in the analysis.

The shape of the return pulse is typically dependent on the direction of its return. Extreme steering angle returns tend to be skewed, and near-vertical angle returns become more symmetric and Gaussian-shaped. Using the method of moments to characterize the shape of the return, we showed this to be true. The shape of the filtered returns fits the symmetric types II, VII, and Gaussian densities of the Pearson system for the near-vertical angles, and fits the skewed type IV density shape at the outer angles. For precise matched filtering techniques, it is desirable then to choose a filter that models this directional nature of the returns. Hence, the Rician pdf, which approximates the Rayleigh pdf at extreme angles and approximates the Gaussian at near-vertical angles, models the nature of the return more accurately than does the Gaussian. Creating a matched filter using the Rician pdf should yield a better result than the Gaussian, and their performance should be compared.

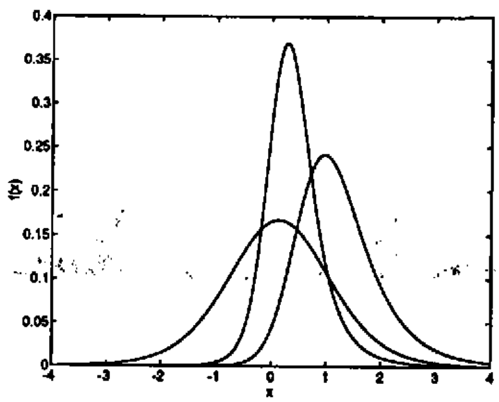

Figure 5: Pearson IV densities.

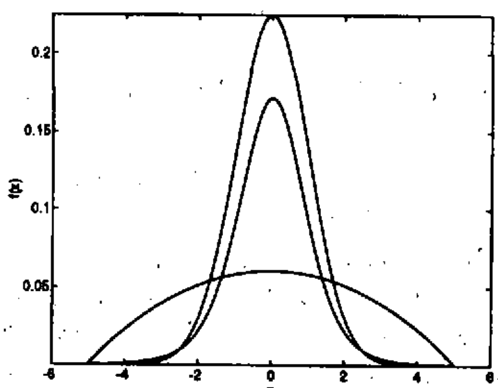

Figure 6: Pearson II/VII densities.

6. ACKNOWLEDGEMENTS

The authors acknowledge the Office of Naval Technology, project element 602435N, managed by Dr. Herbert C. Eppert, Jr., NRL, Stennis Space Center, MS. This paper, NRL Contribution Number PR 92:116:351, is approved for public release; distribution is unlimited.

References

[1] S. D. Morgera and R. Sankar, "Digital signal processing for precision wide-swath bathymetry," *IEEE Journal of Oceanic Engineering*, vol. 9, no. 2, pp. 73–84, 1984.

[2] E. J. Kaminsky, B. S. Bourgeois, A. B. Martinez, and H. S. Barad, "SASS imagery development," 1992. Unpublished.

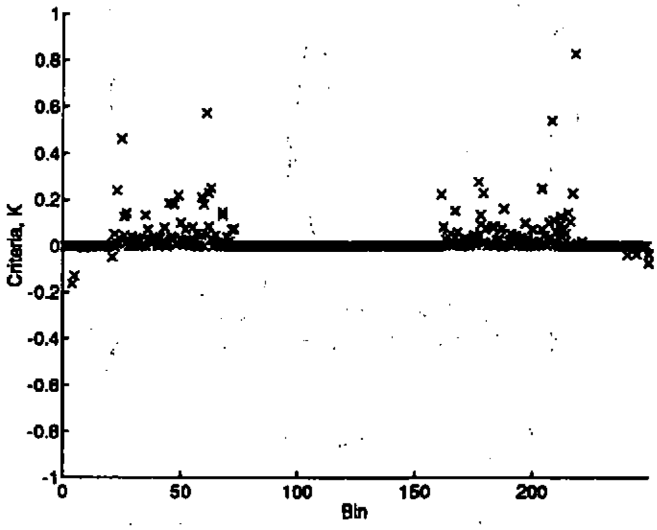

Figure 7: Criteria κ of filtered SASS data.

[3] S. D. Morgera, "Signal processing for precise ocean mapping," *IEEE Journal of Oceanic Engineering*, vol. 1, no. 2, pp. 49–57, 1976.

[4] E. Kaminsky, A. Martinez, B. Bourgeois, C. Zabounidis, and J. Capell, "Determination of the time of Energy Return from Beamformed Data," in *Proceedings of the Conference for Acoustic Classification and Mapping of the Seabed*, (University of Bath, UK), April 14-16 1993.

[5] V. Ol'shevskii, *Characteristics of Sea Reverberation*. New York: Consultants Bureau, 1967.

[6] A. B. Martinez and J. B. Thomas, "Detector design using a density fit to non-gaussian noise," *IEEE Transactions on Information Theory*, vol. 34, no. 3, pp. 544–550, 1988.